Electronic Supplementary Material (ESI) for Journal of Materials Chemistry A.

Supplementary Information

Hydrated $NH_4V_3O_8$ Nanobelts Electrode for Superior Aqueous and Quasi-Solid-State Zinc Ion Batteries

Jianwei Lai,[†] Hui Tang,[‡] Xiuping Zhu,[§] Ying Wang[†]*

[†] Department of Mechanical & Industrial Engineering, Louisiana State University, Baton Rouge, LA 70803, USA.

[‡] School of Materials and Energy, University of Electronic Science and Technology, Chengdu, 610000, China.

[§] Department of Civil and Environmental Engineering, Louisiana State University, Baton Rouge, LA 70803, USA.

* Corresponding author: Prof. Ying Wang, E-mail: ywang@lsu.edu.

Synthesis Method

$NH_4V_3O_8 \cdot 1.9H_2O$ (AVO-1) was synthesized through a hydrothermal method. In a typical synthesis, 1 g commercial V_2O_5 power was added into 5 mL ammonium hydroxide (28-30%). Subsequently, 40 mL of 0.1 M oxalic acid was added into the above solution, and the mixed solution was stirred for 30 min at room temperature. Later, the pH of the solution was adjusted to 3 by dropwise adding the hydrochloric acid (36%). Then, the solution was transferred into a 100 mL Teflon-lined autoclave and kept at 190 °C for 5 h. Finally, the product, AVO-1 was collected, washed with deionized water and ethanol several times, and then dried at 60 °C overnight. $NH_4V_4O_{10} \cdot 1.6H_2O$ (AVO-2) was synthesized by the same procedure, except for adding 40 mL of 0.2 M oxalic acid.

The quasi-solid-state electrolyte was prepared by the following procedure: 1g gelatin power was mixed with 5 mL of 1 M $ZnSO_4$ aqueous solution and kept stirring at 75 °C for 3 h. Later, the mixed solution was poured on a silicon wafer at room temperature to achieve the gel, which serves as the gel electrolyte.

Materials characterization

The X-ray diffraction (XRD) data were collected at a constant scanning rate of 2° min^{-1} on a Rigaku MiniFlex X-ray diffractometer with Cu Kα radiation (λ = 1.5405 Å). Scanning electron microscopy (SEM) imaging was carried out on a FEI Quanta 3D FEG field emission scanning electron microscopy (FESEM). Transmission electron microscopy (TEM) and high-resolution TEM (HRTEM) imaging was performed on a JEOL JEM-2010 microscope at 200 kV. X-ray photoelectron spectroscopy (XPS) measurements were recorded by an AXIS165 spectrometer. Thermogravimetry (TG) data were collected using an SII STA7300 analyzer under the nitrogen atmosphere.

Electrochemical characterization:

The working electrode was fabricated by rolling 60 wt% active material, 30 wt% conductive carbon (Super P), and 10 wt% polytetrafluoroethylene (PTFE) into thin film. For the aqueous batteries, Zinc foil, 3 M zinc trifluoromethanesulfonate ($Zn(CF_3SO_3)_2$) or $ZnSO_4$ aqueous solution, and glass fiber membrane were used as the anode, electrolyte, and separator, respectively, which were assembled in 2032 coin-type cells. For the quasi-solid-state batteries, flexible Zinc foil and gelatin/$ZnSO_4$ gel electrolyte were employed as anode and electrolyte, correspondingly. Galvanostatic charge-discharge experiments were carried out on an eight-channel battery analyzer (MTI corporation) with a voltage range of 0.2- 1.4 V. Cyclic voltammetry measurements and Electrochemical Impedance Spectroscopy was conducted on an electrochemical workstation (CHI 6504C) with a frequency range from 100 kHz to 0.01 Hz. Galvanostatic intermittent titration technique (GITT) measurements were operated on a potentiostat (VMP3, Bio-Logic). Before the GITT measurement, the assembled cell was first discharged and charged at 100 mA g^{-1} for one cycle to obtain a stable state. Subsequently, the assembled cell was discharged or charged at 50 mA g^{-1} for 30 min, and then rested for 60 min to make the voltage reach the equilibrium. The procedure was repeatedly applied to the cell during the entire charge-discharge process until reaching to the cut-off voltage (0.2 / 1.4 V).

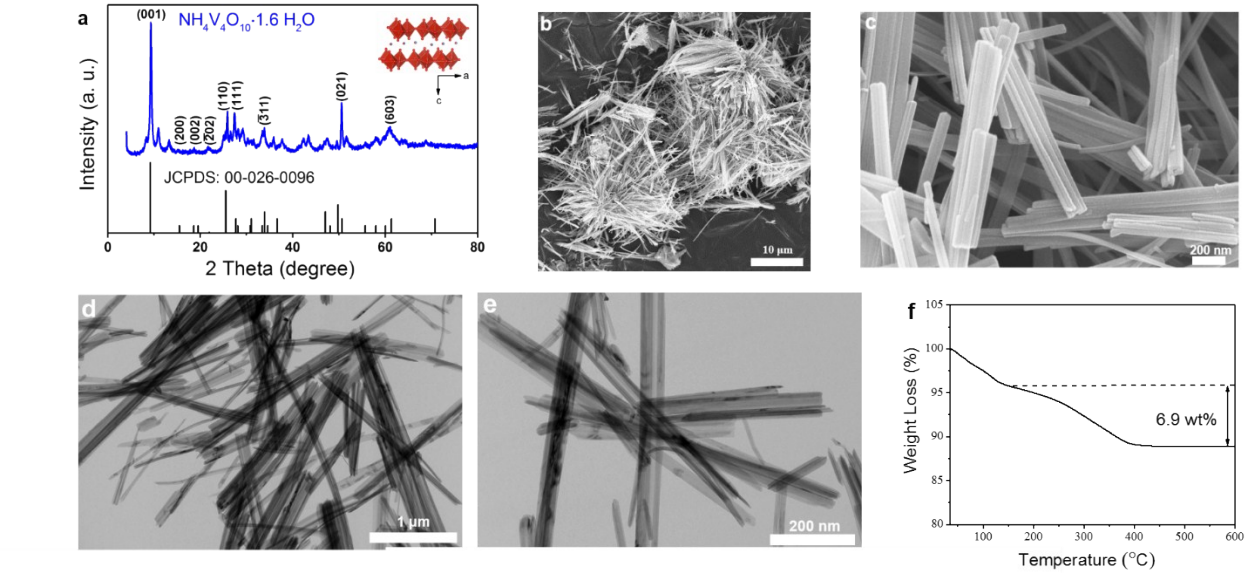

Figure S1. (a) XRD pattern and the inset showing the crystal structure, (b-c) SEM images, (d-e) TEM images, and (f) TGA result of the AVO-2.

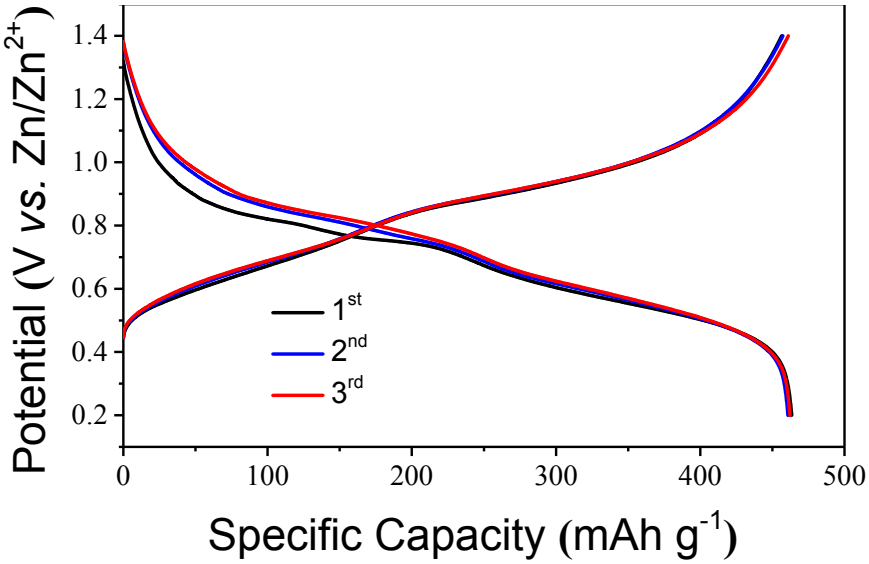

Figure S2. Discharge-charge profiles of the AVO-1 electrode at 0.1 A g^{-1}.

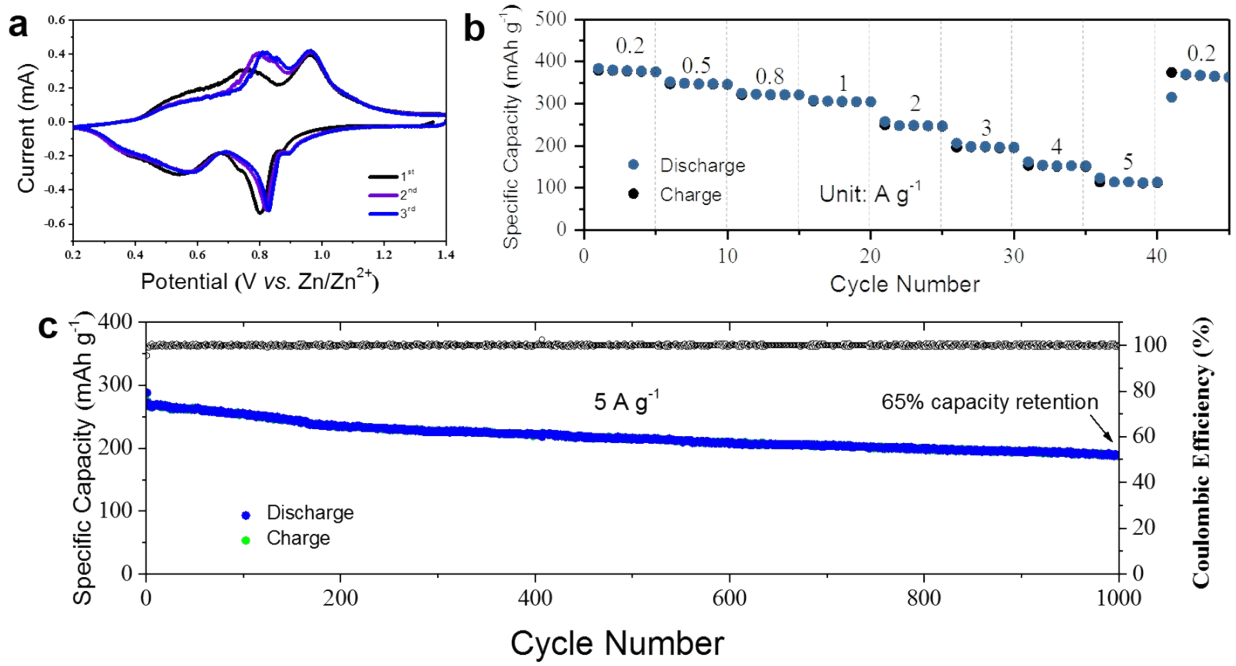

Figure S3. (a) CV curves at a scan rate of 0.1 mV s^{-1} in the initial three cycles, (b) rate performance, and (c) long-term cycling performance at the current density of 5 A g^{-1} of the AVO-2 electrode.

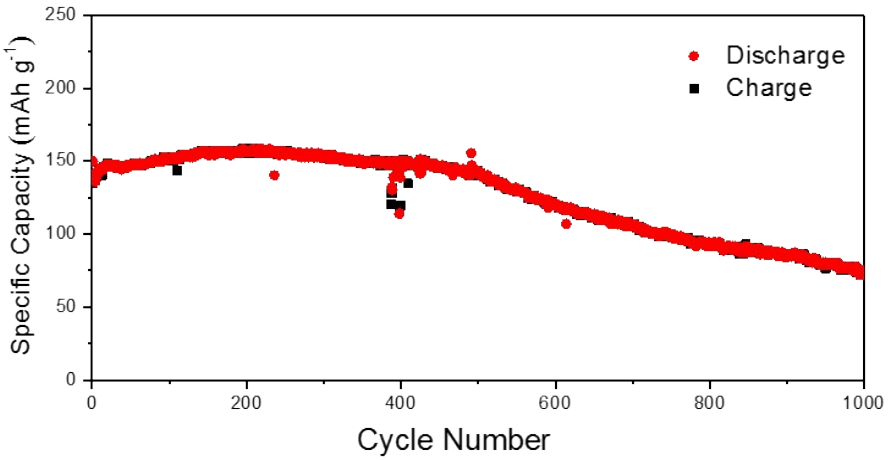

Figure S4. Cycling property of AVO-1 employing 3M $ZnSO_4$ aqueous electrolyte in the voltage range of 0.2-1.4 V at 5A g^{-1}.

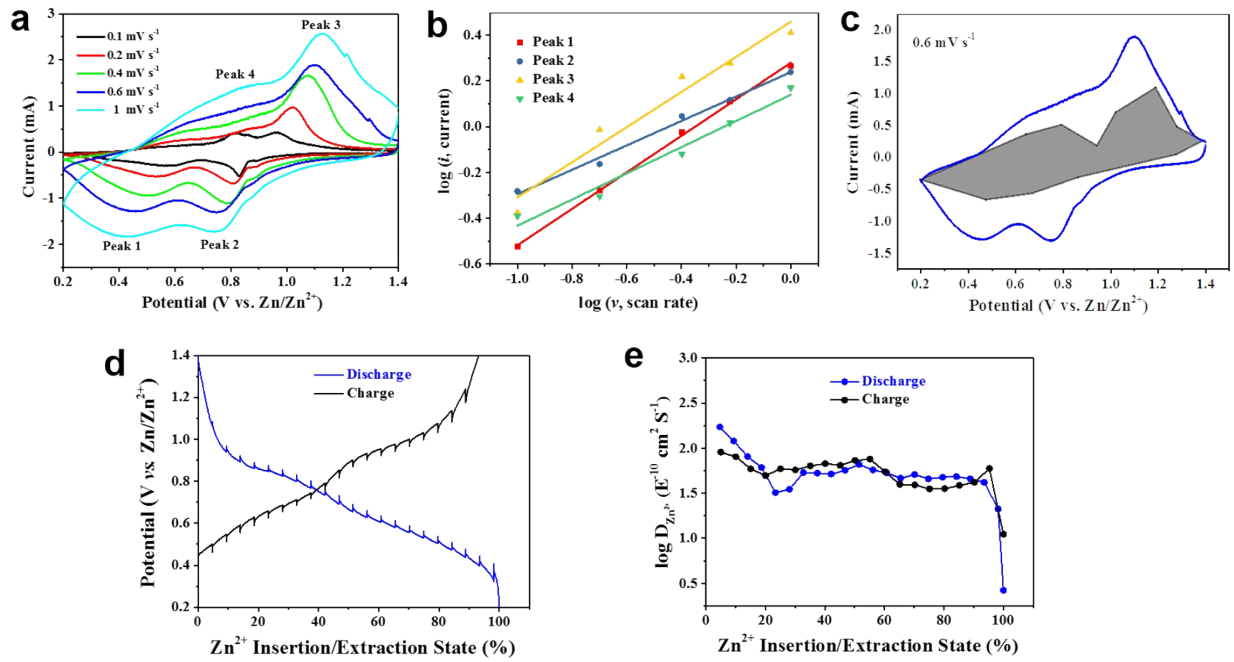

Figure S5. (a) CV profiles of the Zn/AVO-2 cell at different scan rates. (b) Log *i* versus log *v* plots at selected reduction/oxidation states based on the CV data. (c) CV curve showing the capacitive contribution (gray area) at 0.6 mV s^{-1}. (d) GITT curves of AVO-2 electrode. (e) Calculated diffusion coefficient of Zn^{2+} *vs.* various Zn^{2+} insertion/extraction states of AVO-2.

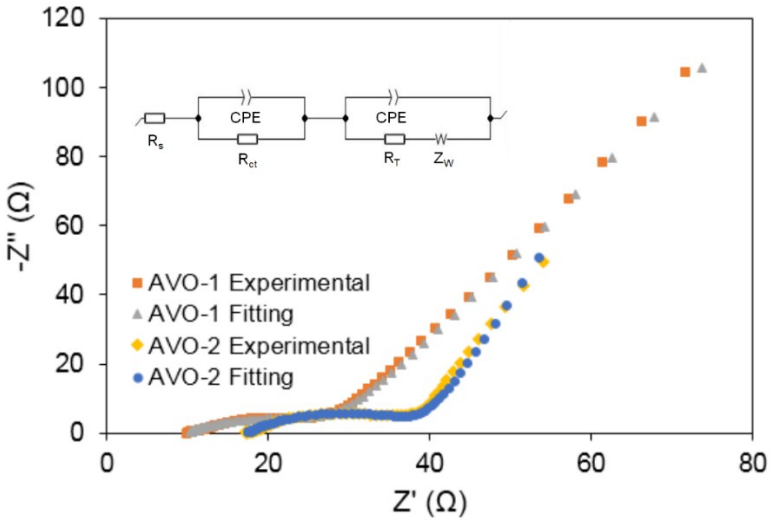

Figure S6. Electrochemical impedance spectroscopy curves of Zn/AVO-1 and Zn/AVO-2 aqueous batteries at the first charged state.

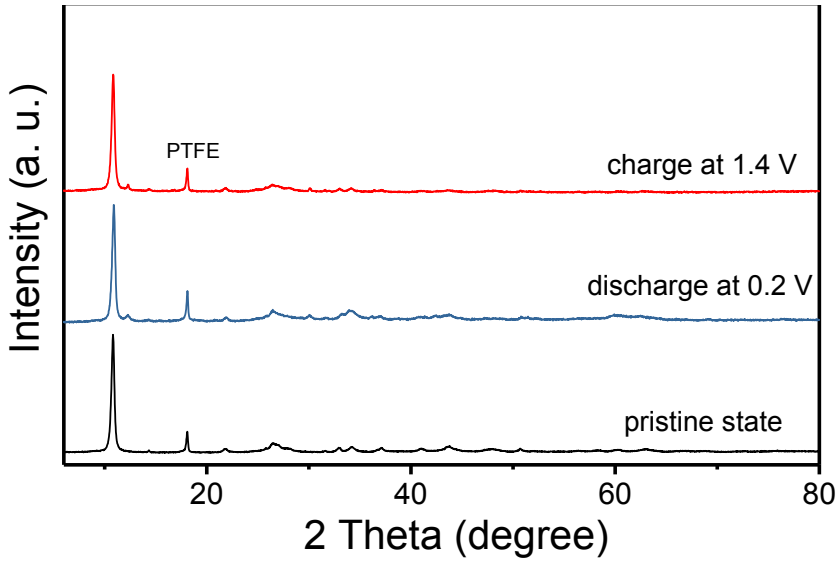

Figure S7. Ex situ XRD patterns of the AVO-1 cathode at various electrochemical states under the current density of 0.2 A g^{-1}.

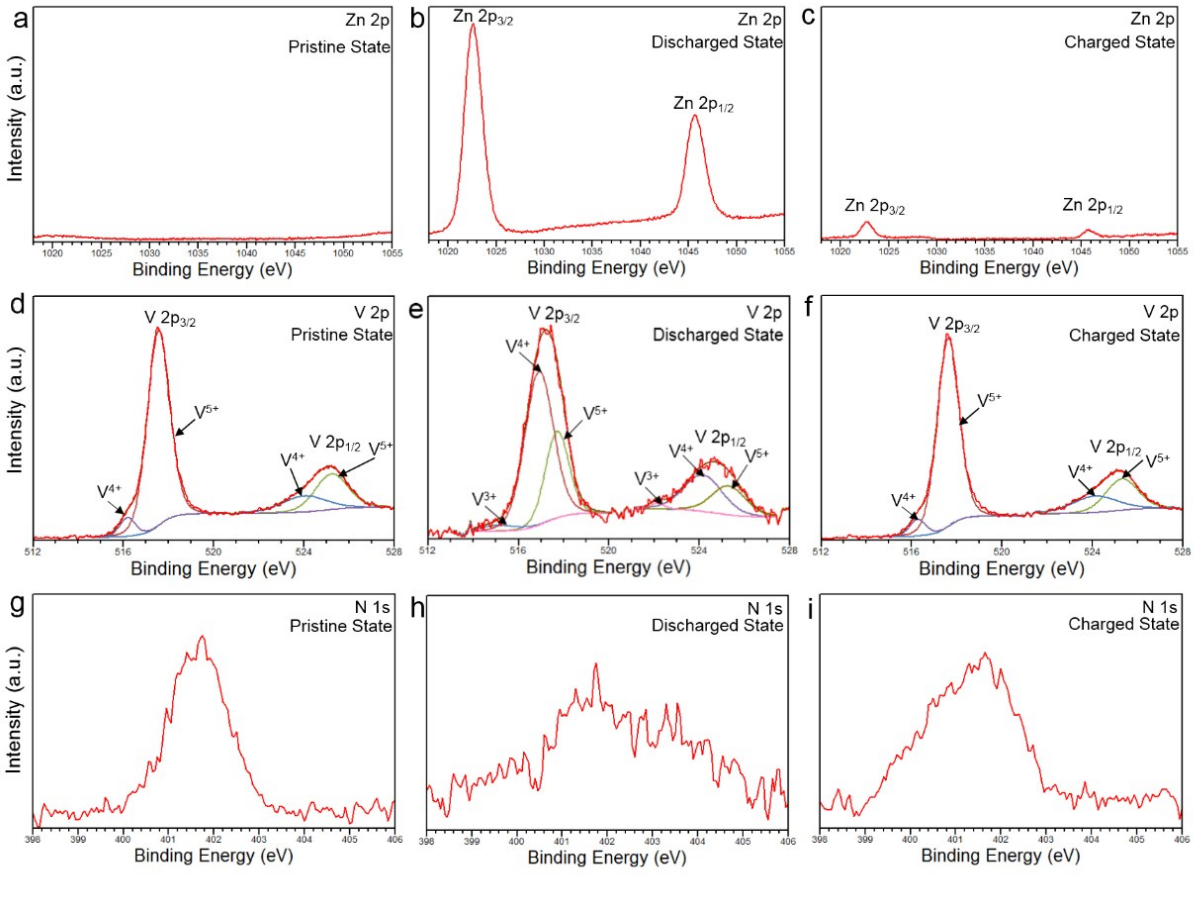

Figure S8. Ex situ XPS spectra of AVO-1 electrodes at various electrochemical states: (a-c) Zn 2p, (d-f) V 2p, (g-i) N 1s at the pristine, fully discharged, and fully charged states, respectively.

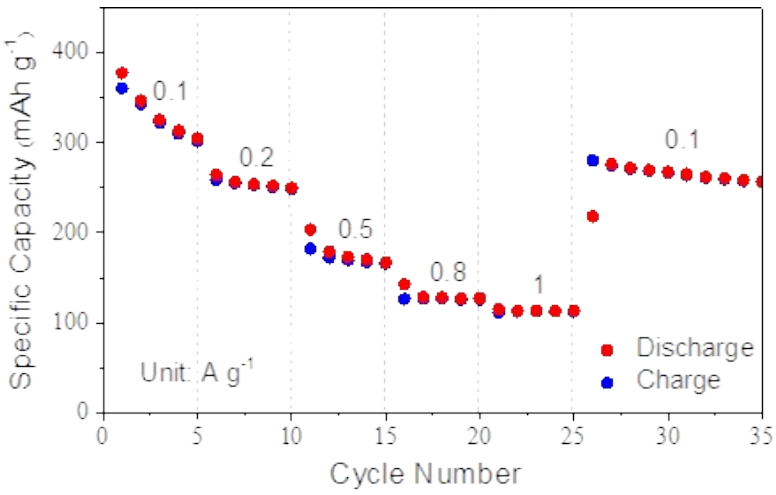

Figure S9. Rate capability of the QSS Zn/AVO-1 battery ranging from 0.1 A g^{-1} to 1 A g^{-1}.

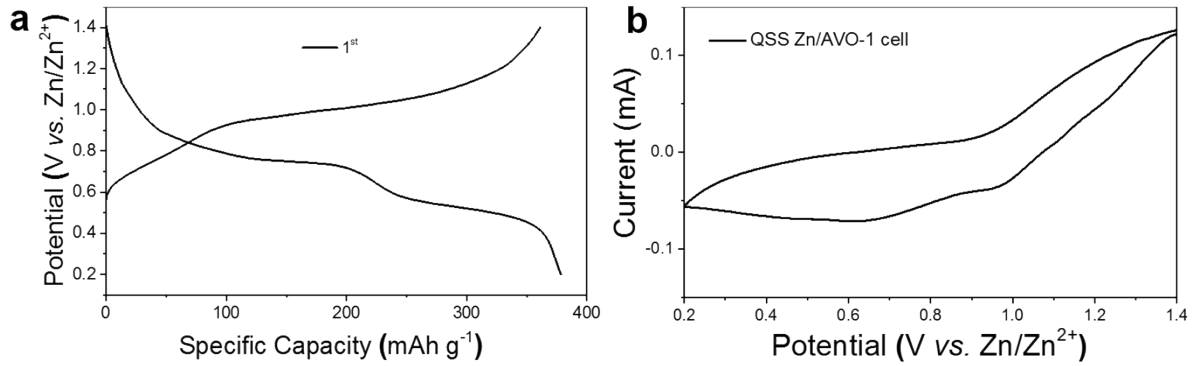

Figure S10. (a) Discharge-charge curves at 0.1 A g^{-1} and (b) CV profile at a scan rate of 0.5 mV s^{-1} of AVO-1 electrode in QSS batteries.

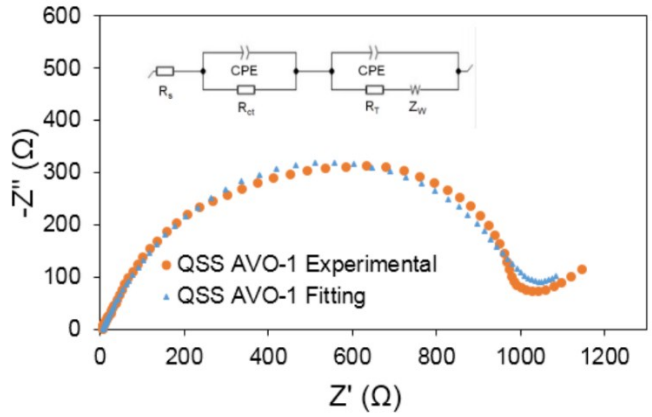

Figure S11. EIS curves of QSS Zn/AVO-1 battery at the first charged state.

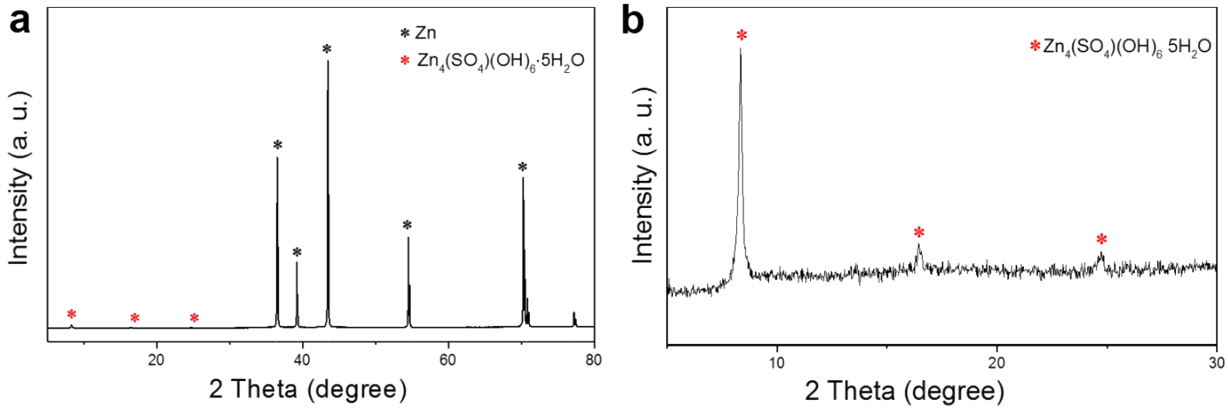

Figure S12. XRD pattern of Zn anode at the first fully discharged state in QSS Zn/AVO-1 cell with 2 theta of (a) 5-80°, (b) 5-30°.

Table S1. Comparison of our work with previous reported vanadium-based cathode materials on the electrochemical performances for aqueous zinc-ion battery.

Electrodes	Specific capacity (mAh g^{-1})/ Current density (mA g^{-1})	Long-term cycling capacity (mAh g^{-1}) after x cycles at y mA g^{-1} with a capacity retention of z	Reference
$NH_4V_3O_8 \cdot 1.9H_2O$	**463/ 100**	**233 (x=1000, y=5000, z=87%)** **166 (x=2000, y=10000, z=81%)**	**Present work**
$V_2O_5 \cdot nH_2O$	381/ 60	200 (x=900, y=6000, z=71%)	1
VO_2 (B)	357/ 100	250 (x=300, y=2000, z=91%)	2
$V_3O_7 \cdot H_2O$	375/ 375	216 (x=200, y=3000, z=80%)	3
$VO_{1.52}(OH)_{0.77}$	140/ 15	105 (x=50, y=15, z=70%)	4
VS_2	190/ 50	111 (x=200, y=500, z=98%)	5
LiV_3O_8	280/ 16	150 (x=65, y=133, z=75%)	6
$Na_{1.1}V_3O_{7.9}$@rGO	238/ 50	171 (x=100, y=300, z=76%)	7
$NaV_3O_8 \cdot 1.35H_2O$	366/ 100	200 (x=200, y=10000, z=100%)	8
$Na_3V_2(PO_4)_3$/C	97/ 50	72 (x=100, y=50, z=74%)	9
$K_2V_8O_{21}$	247/ 300	208 (x=300, y=6000, z=83%)	10
$Zn_{0.25}V_2O_5 \cdot nH_2O$	300/ 50	208 (x=1000, y=2400, z=80%)	11
$Zn_3V_2O_7(OH)_2 \cdot 2H_2O$	213/ 50	101 (x=300, y=200, z=68%)	12

References

1. M. Yan, P. He, Y. Chen, S. Wang, Q. Wei, K. Zhao, X. Xu, Q. An, Y. Shuang, Y. Shao, K. T. Mueller, L. Mai, J. Liu and J. Yang, *Adv. Mater*., 2018, **30**, 1703725.
2. J. Ding, Z. Du, L. Gu, B. Li, L. Wang, S. Wang, Y. Gong and S. Yang, *Adv. Mater*., 2018, **30**, 1800762.
3. D. Kundu, S. H. Vajargah, L. Wan, B. Adams, D. Prendergast and L. F. Nazar, *Energy Environ. Sci*., 2018, **11**, 881-892.
4. J. H. Jo, Y-K. Sun and S-T. Myung, *J. Mater. Chem. A*, 2017, **5**, 8367-8375.
5. P. He, M. Yan, G. Zhang, R. Sun, L. Chen, Q. An and L. Mai, *Adv. Energy Mater*., 2017, **7**, 1601920.
6. M. H. Alfaruqi, V. Mathew, J. Song, S. Kim, S. Islam, D. T. Pham, J. Jo, S. Kim, J. P. Baboo, Z. Xiu, K-S. Lee, Y-K Sun and J. Kim, *Chem. Mater*., 2017, **29**, 1684-1694.
7. Y. Cai, F. Liu, Z. Luo, G. Fang, J. Zhou, A. Pan and S. Liang, *Energy Storage Mater.*, 2018, **13**, 168-174.
8. Z. Xie, J. Lai, X. Zhu and Y. Wang, *ACS Appl. Energy Mater*., 2018. **1**, 6401-6408.
9. G. Li, Z. Yang, Y. Jiang, C. Jin, W. Huang, X. Ding and Y. Huang, *Nano Energy*, 2016, **25**, 211-217.
10. B. Tang, G. Fang, J. Zhou, L. Wang, Y. Lei, C. Wang, T. Lin, Y. Tang and S. Liang, *Nano Energy*, 2018, **51**, 579-587.
11. D. Kundu, B. D. Adams, V. Duffort, S. H. Vajargah and L. F. Nazar, *Nat. Energy*., 2016, **1**, 16119.
12. C. Xia, J. Guo, Y. Lei, H. Liang, C. Zhao and H. N. Alshareef, *Adv. Mater*., 2018, **30**, 1705580.